Enhancement of Coastal Flood Inundation Forecasting by Implementing Downscaling Techniques on the ADCIRC+SWAN Outputs using Kalpana

By

Raam Balaji V, Sandhya K G, Mahendra R S, Francis P A, P C Mohanty

Indian National Centre for Ocean Information Services (INCOIS)

Earth System Science Organization (ESSO)

Ministry of Earth Sciences (MoES)

Hyderabad, India

October 2024

Abstract:

Effective prediction of coastal flooding and associated inundation caused by extreme weather events, such as cyclones and high waves or swells, is critical for coastal hazard mitigation and emergency response planning. A fully coupled ADCSWAN model (ADvanced Circulation + Simulating WAves Nearshore), which uses unstructured grids, is utilized to simulate wave-induced flooding during Southern Ocean swell events. Although the model is capable of capturing swell surge along the coastline, its coarse mesh resolution limits the accurate representation of inundation extent, as the mesh size exceeds the spatial scale of the flooding. Developing high-resolution meshes across extensive coastal regions introduces computational challenges, significantly increasing model runtime and delaying emergency planning efforts. To overcome this, post-processing techniques are applied to medium/coarse-resolution parent meshes to enhance spatial resolution, making this approach more feasible for operational use.

This study explores the downscaling capabilities of Kalpana, a Python module that transforms ADCIRC output into geographic vector formats and specifically downscales maximum water elevations into finer-resolution rasters. Two downscaling methods are investigated: the Static Method and the Head Loss Method. The Static Method, which extends the same water level inland, is computationally efficient but tends to overestimate flood extents by disregarding land cover friction. In contrast, the Head Loss Method accounts for energy losses due to land cover friction, resulting in more accurate flood predictions; however, it requires detailed land cover data and calibration of friction parameters.

This study performs a comprehensive evaluation of the methodologies using sample inputs from Kalpana's tool repository, demonstrating the implementation and comparative performance of each method. Furthermore, we extend the application of this tool to downscale swell wave-induced flooding, utilizing a high-resolution Digital Elevation Model (DEM) and land cover datasets for the Kerala region. The results indicate that while the Static Method is simpler and faster, the Head Loss Method provides superior accuracy, making it more suitable for precise flood risk assessments. The practical utility of these downscaling techniques is further emphasized by the development of a user-friendly Graphical User Interface (GUI) application, achieved through the integration of separate codes into a unified script.

Enhancement of Coastal Flood Inundation Forecasting by Implementing Downscaling Techniques on the ADCIRC+SWAN Outputs using Kalpana

By

Raam Balaji V, Sandhya K G, Mahendra R S, Francis P A, P C Mohanty

Indian National Centre for Ocean Information Services (INCOIS)

Earth System Science Organization (ESSO)

Ministry of Earth Sciences (MoES)

Hyderabad, India

October 2024

Acknowledgments

Author Contributions

RBV and SKG together conceived the idea and designed the study framework. RBV conducted the experiments, generated the model mesh for Kerala, conducted model simulations, plotted the figures, and prepared the first draft of this manuscript. RBV and SKG together analyzed the model outputs and drawn conclusions. SKG provided the wave boundary conditions for the Kerala model runs. MRS and PCM blended the bathymetric and topographic data sets available at INCOIS, resampled to required resolution and smoothened as per model requirement. SKG and FPA provided the necessary technical support and guidance and edited the manuscript.

Table of contents

LIST OF FIGURES

NOTATIONS

n   Manning's coefficient

h_L head loss

L   Lateral distance between cell centers

U   Flow velocity

k   Unit conversion factor

R   Hydraulic radius

ABBREVIATIONS

Maxele	Maximum Water Surface Elevation
GUI	Graphical User Interface
ALTM	Airborne LiDAR Terrain Mapping
ADCSWAN	ADCIRC+SWAN
ADCIRC	Advanced Circulation
2DDI	Two-dimensional Depth Integrated
SWAN	Simulating Waves Nearshore
WGS84	World Geodetic System 1984
DEM	Digital Elevation Model
LULC	Land Use/Land Cover
CRS	Coordinate Reference System
HPC	High-Performance Computing
SRTM GL1	Shuttle Radar Topography Mission Global 1 arc-second
UTM	Universal Transverse Mercator
r.grow	Command for growing raster areas
r.walk	Command for calculating movement and pathfinding
CSV	Comma-Separated Values
epsgIn	EPSG code for input coordinate system
epsgOut	EPSG code for output coordinate system
vUnitIn	Vertical unit for input data
vUnitOut	Vertical unit for output data
exportMesh	Function to export mesh data
repLenGrowing	Parameter for representative length growth factor
floodDepth	Function to convert water levels to water depth
finalOutToLatLon	Function to reproject the final output to latitude/longitude
ras2vec	Function to export results as vector files
img	Erdas Imagine
createGrassLocation	Function to create a GRASS GIS location

createLocMethod   Function to specify the method for creating GIS location

waterClass   Classification of water types

minArea   Minimum area threshold for analysis

slopeFactor   Factor related to slope adjustments

walkCoeefs   Coefficients used in walking or pathfinding algorithms

level   For setting the contour levels

subDomain   A specific subset of a larger domain for analysis

epsgSubDom   EPSG code for the coordinate system of a subdomain

zeroDif   Zero difference threshold

1. INTRODUCTION

1.1 Motivation

Tropical cyclones and high wave/swell events present significant threats to coastal regions by inducing flooding that endangers coastal infrastructure and human safety. While well-established modeling systems exist for simulating cyclone-induced flooding, a standardized methodology for predicting swell wave-induced flooding and associated inundation is lacking. A swell event, characterized by the accumulation of high-energy, long-wavelength waves originating from distant weather systems, results in water piling up along the coast. Kerala is particularly vulnerable to such events, as demonstrated by significant flooding occurrences in 2016, 2018, 2019, and 2024.

In India, disaster management relies on the INCOIS warning system, which uses the data-assimilated WAVEWATCH III model for forecasting these waves. However, the modeling system for swell surges and associated flooding has not yet been fully implemented. Presently, in experimental mode, a coupled model approach is employed, where ADCIRC addresses hydrodynamic aspects, and SWAN, in conjunction with WAVEWATCH III, takes care of the effect of waves. Given that swell events are micro-scale phenomena, accurately modeling their surge and associated inundation with low-resolution global relief data presents challenges. To address these limitations, a coastal relief model developed by INCOIS, with a spatial resolution of 30 meters, was used. This model integrates bathymetric data collected using a single beam echo sounder from various institutes, along with topographic data derived from Airborne LiDAR Terrain Mapping (ALTM) surveys and Cartosat satellite observations. It has been employed for mesh generation to accurately capture flow interactions with detailed coastal features.

For the Kerala coast, the model has been configured with a 100-meter mesh resolution near the shoreline. However, this resolution remains inadequate to accurately capture inundation extents less than 100 meters. While increasing the mesh resolution would enhance accuracy (Westerink et al., 2008), it would also prolong forecasting time, presenting a trade-off between accuracy and computational efficiency (Bunya et al., 2010; Cyriac et al., 2018; Dietrich et al., 2011; Graham et al., 2017). Geospatial post-processing techniques using Kalpana tool (https://ccht.ccee.ncsu.edu/downscaling-flooding-inundation-extents-using-kalpana/) allow for the enhancement of flood prediction resolution without the need for further mesh refinement

(Tull, 2018). This process enhances the precision of inland maximum water surface elevation estimates (maxele.63.nc) by applying fundamental physical principles. Kalpana employs two primary techniques: the Static Method, which utilizes water surface elevation and topographic DEM data for downsizing, and the Head Loss Method, which incorporates land classification data to account for frictional losses as flow traverses different resistance zones.

Chapter 2 explains the modeling framework and downscaling techniques, while also validating the Kalpana installation using sample data to ensure all modules are functional for downscaling tasks. It covers the necessary file inputs, and parameter tuning. Chapter 3 assesses the effectiveness of each downscaling method within the context of swell surge inundation scenarios. Finally, Chapter 4 summarizes the key findings and offers recommendations for future research.

1.2 Objectives

The primary objective of this study is to enhance the accuracy of coastal flooding inundation forecasting by applying downscaling techniques to ADCIRC flood inundation predictions. To achieve this, the study encompasses the following technical tasks:

a) Install and configure the Kalpana tool on the computational system to enable the downscaling process.

b) Conduct a detailed evaluation of input data requirements and downscaling methodologies by running a tutorial case focused on downscaling storm-induced flooding.

c) Set up and assess a coupled ADCSWAN model for the Kerala coast to evaluate the effectiveness of Kalpana's downscaling approach in scenarios of swell wave-induced flooding inundation.

2. MODELING SYSTEM AND SOFTWARE USED

2.1 Swell Surge Inundation Forecasting using Coupled ADCSWAN Model

Swell surge refers to the elevated coastal water levels caused by the arrival of long-wavelength, high-energy waves, typically generated by distant meteorological systems. The Indian coastline, along the Arabian Sea (AS) and the Bay of Bengal (BoB), is highly susceptible to swell events originating from the Southern Indian Ocean (SIO). As these swells propagate towards the coast, they can be further amplified upon encountering opposing coastal currents, leading to increased water levels and a heightened risk of coastal inundation. This risk is particularly severe in low-lying regions, where the combined effects of wave setup and coinciding spring tides exacerbate the flooding potential.

Effective forecasting of coastal water levels during swell events requires a comprehensive approach that accounts for the dynamic interactions among tidal forces, wave propagation, coastal currents, and overland flood dynamics. The coupled ADCSWAN model offers a robust solution by integrating hydrodynamic and spectral wave models, facilitating the simulation of coastal responses to swells and other forcing conditions. The following sections will provide an overview of ADCIRC, SWAN, and the advantages of coupling these models.

2.1.1 ADCIRC

ADCIRC serves as the primary hydrodynamic model in this study, with a focus on simulating tidal dynamics. It is further enhanced by its capability to incorporate wind-driven water level adjustments and its integration with wave models. Additionally, its ability to account for wetting and drying processes in areas with large intertidal zones or regions prone to periodic flooding strengthens its applicability. ADCIRC operates using the finite element method, which enables the use of flexible, unstructured grids. The model applies two-dimensional depth-integrated shallow water equations (ADCIRC-2DDI), solving generalized wave continuity equations for water levels and vertically integrated momentum equations for current velocities at each computational point and time step (Luettich et al., 2004).

2.1.2 SWAN

SWAN is a third-generation spectral wave model designed exclusively to simulate surface gravity waves in coastal and near-shore waters. It solves the wave action balance equation,

which accounts for wave generation, propagation, dissipation, and non-linear interactions between waves (Booij et al., 1999). SWAN has the structured grid and unstructured grid options. The unstructured grid option is particularly advantageous for regions with irregular coastlines or varying depths, ensuring a high level of detail in wave simulations (Zijlema, 2010). It has the ability to incorporate boundary conditions from the global WAVEWATCH III model. This feature allows SWAN to include remotely generated swell waves in its simulations, particularly those originating in distant regions like the Southern Indian Ocean.

2.1.3 ADCSWAN

ADCIRC, dynamically coupled with the SWAN model, has undergone extensive validation for its effectiveness in surge modeling applications [Dietrich et al., 2011, 2012]. Both models share the same unstructured mesh and exchange information at specified coupling intervals. ADCIRC initially computes water surface elevations and currents using spatially and temporally interpolated wind fields mapped to the computational grid. This data is then transferred to SWAN, which computes the wave spectrum based on the wave action density balance equation. The resulting radiation stress from surface gravity waves is subsequently fed back into ADCIRC to improve predictions of water levels and currents. This iterative coupling process allows for an accurate representation of the combined hydrodynamic and wave interactions. A key advantage of the coupled model is its ability to incorporate wave setup into ADCIRC's total water surface elevation, enabling accurate prediction of wave-induced flooding.

2.2 Kalpana Software: Downscaling ADCIRC Output

Although the ADCIRC+SWAN coupled model successfully simulates coastal inundation by incorporating the influence of gravity waves into the ADCIRC maximum water level (maxele.63.nc) output, additional refinement is required to improve accuracy. Achieving meter-scale, high-resolution forecasts essential for disaster management remains challenging with direct numerical model outputs. Kalpana, a post-processing tool, enhances forecast accuracy by employing downscaling techniques to transform raw ADCIRC data into high-resolution inundation maps, enabling clearer visualization of flood risks (Rucker et al., 2021). Kalpana uses the World Geodetic System 1984 (WGS84) as the horizontal datum, enabling compatibility with any ADCIRC mesh globally. By converting mesh data into shapefiles, Kalpana eliminates regional and mesh-specific limitations typically associated with

downscaling processes.

2.3 Geospatial Downscaling Methods

In this study, we evaluate two downsizing techniques: (1) the Static method, where water levels are extended horizontally until they align with the ground surface (Figure 2.1a), and (2) the Head-Loss method, utilizing a land cover dataset to factor in energy dissipation due to friction as water flows over different types of terrain (Figure 2.1b).
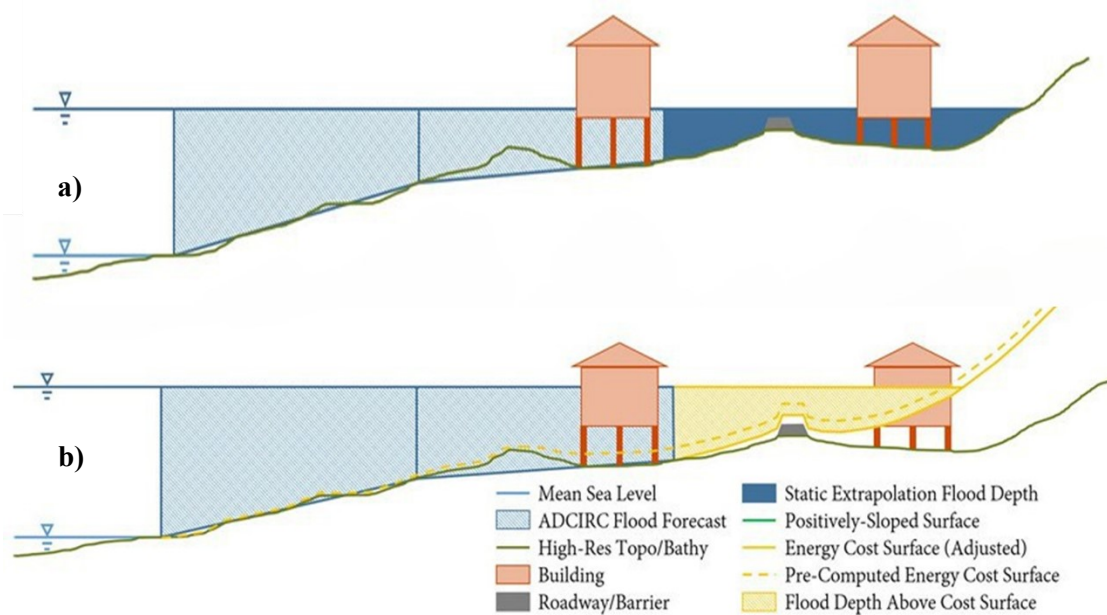
Figure 2.1. Schematic sketch illustrating the outputs from (a) Static method and (b) Head-Loss method (Source: Rucker et al., 2021).

2.3.1 Static Method

In the static approach, the inundation extent derived from the ADCIRC output (maxele.63.nc) undergoes refinement through several procedural stages. Initially, the maximum water surface elevation is scaled down from mesh nodes to a raster at a fine resolution identical to the Digital Elevation Model (DEM). This raster depicting maximum water surface elevation is subsequently expanded uniformly until it meets with the ground surface defined by the DEM. This process utilizes the GRASS GIS module r.grow (Larson & Clements, 2008), which extends the water-level raster into adjacent areas with no data using a specified radius, ensuring that flooded regions are expanded only where water contacts the land surface. Typically, the radius is set to 30 cells (approximately 450 m), reflecting element sizes along the wet/dry

interface (Rucker et al., 2021). Adjustments to this parameter are made based on mesh resolution and local topography. Following extrapolation, a hydraulic connectivity criterion is imposed to mitigate isolated wet cells that may arise from the extension process. GRASS GIS tools such as r.clump, r.reclass, and r.mapcalc are employed to identify and eliminate these isolated areas (Shapiro & Metz, 2008; Westerveldt & Shapiro, 2008; Shapiro & Clements, 1991). This method effectively extends the inundated area to locations where water levels align with the topography, offering a more accurate simulation of inundation dynamics across diverse terrain features such as barrier islands.

2.3.2 Head-Loss Method

In the head-loss approach, the downscaling process incorporates land cover data to adjust flood extents. This adjustment accounts for frictional dissipation influenced by different land cover types. Rather than projecting water surface elevation onto a topography, this technique projects them onto an energy cost surface, which accounts for the combined energy requirements (elevation + head loss) to reach a specific inundation extent. The friction due to land cover is quantified using Manning's coefficient (n), which is derived from the Land Cover Database. An adapted version of Manning's equation is employed to directly compute head loss in surface water flow (Rubin & Atkinson, 2001):

$$h_L = L\left(\frac{nU}{kR^{2/3}}\right)^2$$

In this equation, h_L represents the head loss, L denotes the lateral distance between cell centers, n is Manning's coefficient, U signifies flow velocity, k is a unit conversion factor, and R stands for hydraulic radius, approximated as flow depth in surface flow. This computes head loss for every grid cell. The GRASS GIS module r.walk pre-calculates an energy cost surface, incorporating potential energy gains from DEM elevation changes and frictional head losses from land cover (GRASS Development Team, 2002). This module creates a raster map that illustrates the cumulative expenditure of energy required to move across different geographic locations. The depicted cost integrates both elevation changes and head losses due to land cover. This process generates a least cost path raster. During downscaling, the total cost raster is created using the raw cost raster, U, and R values from ADCIRC forecasts and the DEM ground surface. The predicted water surface is then extended to the energy surface defined by the total cost raster.

2.4 Assessment of Kalpana's Downscaling Methods

To initiate the downscaling process, it is essential to configure the environment for Kalpana and install all required dependencies. Moreover, setting up the GRASS GIS software is necessary. The detailed procedure for these steps is outlined in Appendix A.1.

The downscaled results, based on Hurricane Florence in 2018, were reproduced using the inputs from Kalpana's tool repository. Analyzing these outcomes is crucial for assessing the merits and demerits of these methodologies, particularly in scenarios where they might overestimate or underestimate flood levels. This evaluation will aid in refining and adapting the methods, and in pinpointing adjustable parameters to enhance the accuracy of flood predictions in our study area.

2.4.1 Input Data and Parameters Overview

The static downscaling method necessitates several input files. Primarily, the ADCIRC mesh file (fort.14) is employed. Additionally, a high-resolution raster DEM file in GeoTIFF format is required to establish a GRASS GIS location and ensure mesh resolution compatibility. Another crucial input is a NetCDF file (maxele.63.nc) containing the maximum water surface elevation variable, which is to be downscaled. Furthermore, an optional vertical datum difference file in CSV format, sourced from tide gauge data, may be utilized to adjust vertical datums. Lastly, a Levee's Shapefile can be included to incorporate levee information, if applicable. The code includes several configurable parameters. The coordinate reference systems (CRS) are specified using the variables *epsgIn* and *epsgOut*, which should be updated with the appropriate EPSG codes for the input and output CRS. Vertical units are defined by *vUnitIn* and *vUnitOut*, with default settings of *m* and *ft*, respectively; these should be modified to match the units of your input and output data. Additional variables to adjust include levels for setting contour levels, *exportMesh* to manage the export of the mesh, *repLenGrowing* for the representative length growth factor, *floodDepth* to convert water levels to water depth, *ras2vec* to export results as vector files, and *finalOutToLatLon* to reproject the final output to latitude/longitude.

In the head loss method, in addition to the mesh and DEM files as used in the static method, additional input files are required. These include land cover data in Erdas Imagine (.img) format, which provides necessary information for determining Manning's roughness coefficients. Furthermore, a Manning landcover file in text format is essential, as it contains

the rules for converting land cover types into Manning's roughness values. Downscaling parameters include *createGrassLocation*, a boolean flag to initiate the creation of a new GRASS GIS location, and *createLocMethod*, which specifies the method for creating the GRASS location. Other parameters encompass *URConstant* and *k* for computing the cost surface, *waterClass* for identifying the water class in the land cover raster, *minArea* for defining the minimum area considered, *res* for specifying the downscaling resolution, *slopeFactor* for the slope adjustment in cost calculation, *walkCoeefs* for the coefficients used in walking cost calculations, and *level* for setting the contour levels applied in downscaling. Export settings to configure include *subDomain* for specifying a shape file or bounding box to crop the domain as needed, *epsgSubDom* for indicating the EPSG code of the subdomain, and *zeroDif* for managing zero elevation differences. These parameters must be customized based on our specific dataset and desired output to perform the downscaling process accurately.

2.4.2 Downscaling Outputs and Results

The static and head loss downscaling methods produce a shapefile as a final output with vector data representing the contours of the downscaled elevation. The head loss method also produces several intermediate raster files, including those for the raw and total cost surfaces. These outputs facilitate a comprehensive understanding of the downscaling process.

The evaluation of the two downscaling methods includes an analysis of their processing time, precision in depicting actual flood extents, and their performance across various regions where inaccuracies are observed. The static downscaling method requires a total execution time of 7.292 minutes for this sample case, making it considerably more resource-intensive than the head loss method, which completes in 1.582 minutes. The head loss method demonstrates enhanced computational efficiency throughout various stages, including data export, contour generation, and post-processing. Therefore, the head loss technique is more appropriate for scenarios demanding rapid processing, especially when managing extensive datasets or working under constrained computational resources. This study includes a visual comparison of the flood area and extent predictions from various downscaling methods against the reference results from Rucker et al. (2021). To quantify the alignment between downscaled outcomes and reference data, the number of filled raster cells is used as a metric. The static method shows the largest discrepancies, particularly overestimating flood areas in flat or gently sloping regions near rivers or coastal areas, such as floodplains (Figure 2.2a) and coastal lowlands (Figure 2.2b, labeled 3). This over-prediction occurs because the static method does

not account for energy dissipation caused by land cover friction.
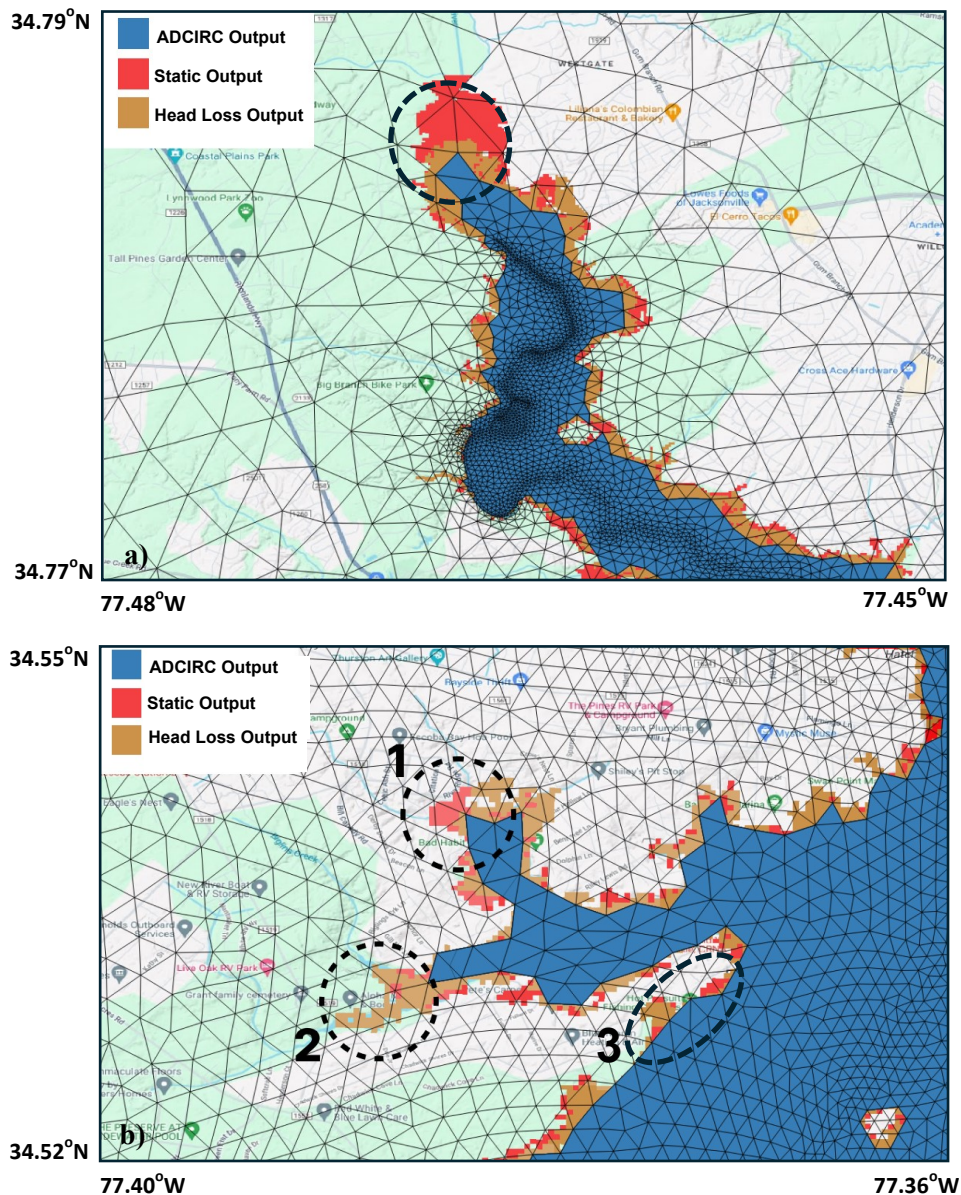
Figure 2.2. Flooding extent in the (a) New River, (b) Chadwick Bay. The ADCIRC model output is represented in blue, static output in red and the head-loss method in mustard yellow.

Although the head-loss method generally offers greater accuracy and alignment with actual conditions, it faces challenges in narrow river sections where limited resolution causes misclassification of land cover types. This misidentification leads to an exaggerated energy dissipation estimation and a consequent underestimation of flood extent (Figure 2.2b, labeled 1). However, in broader inland river zones, the head-loss method performs well by correctly associating the waterbody with its corresponding land cover type. This enables precise friction

calculations and more accurate flood extent predictions (Figure 2.2b, labeled 2). In these regions, where floodplains are absent, the static method also provides reliable results, matching the flood extents predicted by the head-loss approach.

In regions like the New River, Chadwick Bay, and the coastal areas, the head-loss method demonstrates close agreement with actual flood extents. However, slight underestimations are observed in riverine zones due to increased friction and energy costs in smaller tributaries. These discrepancies can be addressed by adjusting friction values or refining perennial features. Overall, the head-loss method is deemed the most accurate for capturing flood dynamics in large river systems, creeks, and coastal lowlands. In contrast, the static method displays notable limitations, including greater computational demand and higher errors. The effectiveness of both methods is largely dependent on the resolution of the ADCIRC mesh, and the quality of the global relief data used for mesh generation.

3. CASE STUDY: SWELL SURGE EVENT ALONG KERALA COAST

3.1 Introduction

This chapter presents a case study aimed at enhancing the accuracy of swell wave-induced flood predictions through the application of the Kalpana. The event is modeled using the ADCIRC+SWAN coupled system, with wave boundary conditions derived from WAVEWATCH III, ensuring precise representation of remotely generated swell wave impacts. The downscaling techniques, specifically the Static and Head-Loss methods, which were originally employed for storm surge events, have been adapted to improve predictions of high tide extents and swell surge inundation. Furthermore, an intuitive GUI has been developed to automate and optimize the downscaling process, enhancing its utility for operational forecasting.

3.2 Background of the Event

The low-pressure system responsible for the coastal flooding alert originated approximately 10,000 km from the Indian coastline in the southern Atlantic Ocean (15°E, 60°S) on April 26, 2024. By April 28, 2024, this system had advanced into the southern Indian Ocean (35–55°E, 60–50°S), generating high-energy swell waves with a period of around 24 seconds. These swells were expected to arrive at the southern tip of India at approximately 21 hrs (UTC) on May 3, 2024. The interaction between these long-period swells and elevated tidal conditions was anticipated to induce coastal flooding in low-lying areas across Lakshadweep, Kerala, South Tamil Nadu, Karnataka, Goa, Maharashtra, Andaman & Nicobar Islands, Odisha, and West Bengal between May 4th and 5th, 2024. INCOIS issued a coastal flooding alert for this event based on WAVEWATCH III model simulations and observational data, highlighting the potential severity of the swell impact.

In addition to this major event, a minor swell surge occurred on March 31, 2024. INCOIS forecasted high-period swell waves with periods ranging from 16 to 19 seconds and issued a rough sea alert for the Kerala coast. Despite being less intense than the May event, these minor swells caused inundation in certain coastal stretches. This event serves as a valuable context for assessing the proposed modeling system's ability to capture varying magnitudes of swell-induced flooding. Following both events, INCOIS conducted a field survey along the heavily impacted Kerala coast, collecting empirical data on maximum swell surge inundation and wave

impacts. This data was utilized in the study to validate the downscaled flood extent analysis, thereby improving the credibility and accuracy of the downscaled model output.

3.3 Generation of the Experimental Mesh for the Kerala Coast

The wavelength-based mesh was generated using the Surface-Water Modeling System (SMS) tool. The scalar paving density method, which incorporates a size dataset derived from the wavelength function, was applied to regulate node spacing and ensure smooth element transitions. This process accurately represents coastal and island topography while minimizing abrupt size changes in the mesh. Two unstructured meshes were employed for this study. The KR-G mesh (Figure 3.1a), developed using GEBCO's 30 arc-second global relief data, covers the entire Kerala coastline. The KR-THR-I mesh (Figure 3.1b) is created with high-resolution (100 m) coastal relief data from INCOIS for the Thrissur coastal stretch.
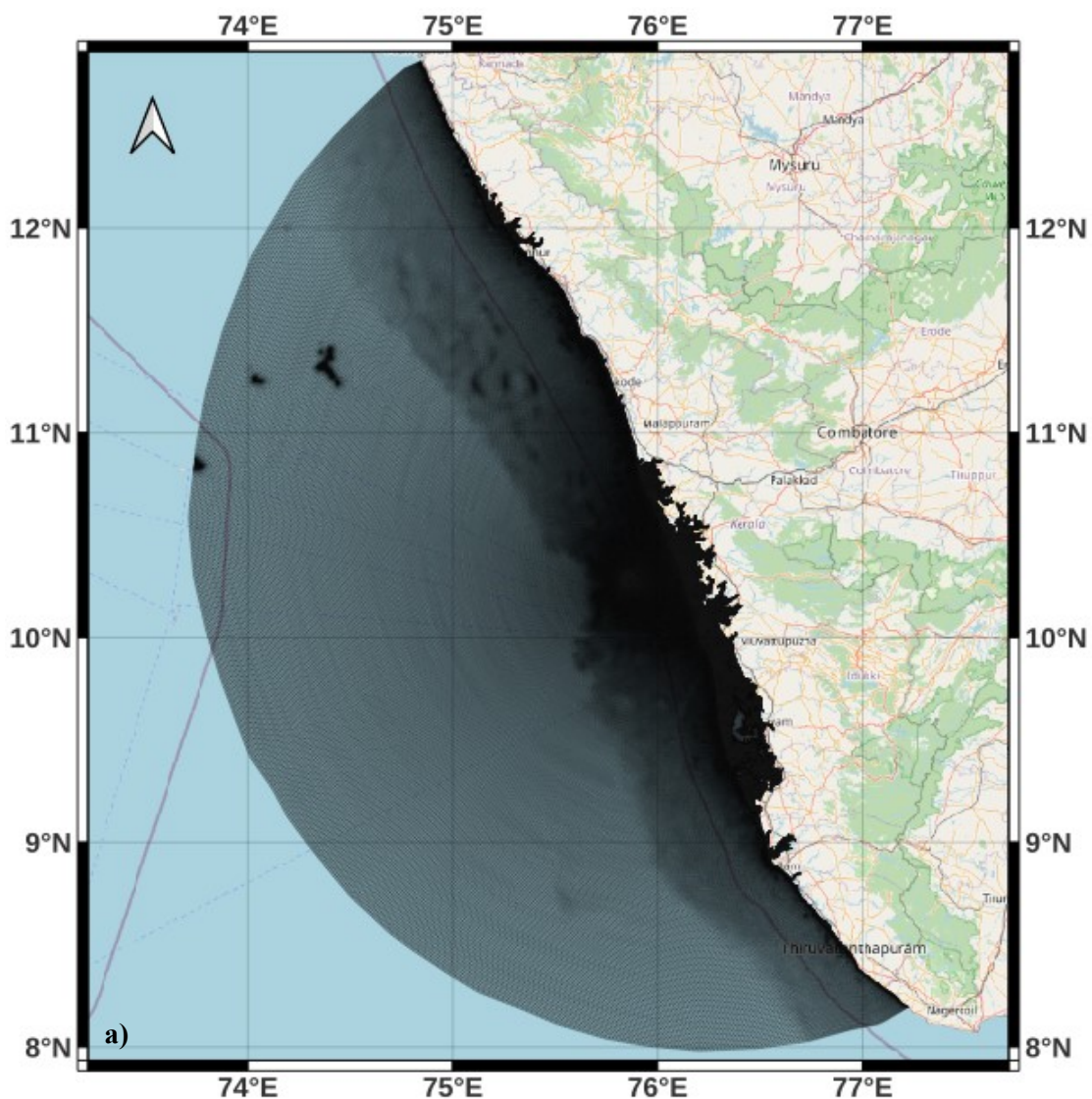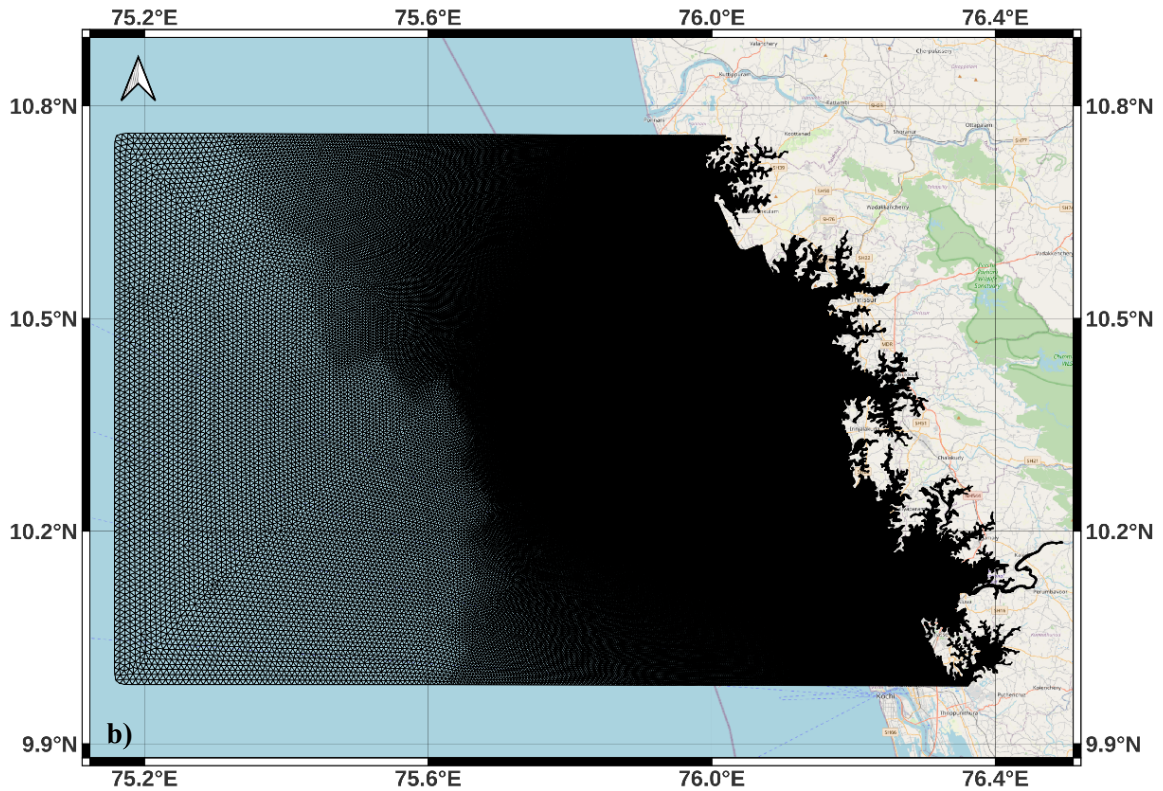
Figure 3.1. Finite Element Mesh for the Kerala Coast: (a) KR-G (based on GEBCO data) and (b) KR-THR-I (covering Thrissur and based on INCOIS data).

Due to processing limitations within SMS, the INCOIS dataset, initially at a 30 m resolution, was resampled to 100 m using QGIS and then employed for mesh creation. To accurately model flood-induced inundation, the land boundary of the experimental mesh was delineated along the 10-meter inland contour. For the KR-G mesh, element sizes range from 5 to 7 kilometers at the open boundaries, tapering to 100 to 150 meters near the coastline. This mesh includes 728,929 nodes and 1,445,261 triangular elements, with increased element density around Thrissur due to a radial distribution strategy (Figure 3.1a). On the other hand, the KR-THR-I mesh has element sizes ranging from 1 to 2 kilometers at the open boundaries and 100 to 150 meters near the coast. It includes 304,955 nodes and 596,281 elements, offering finer coastal details but requiring more computational resources (Figure 3.1b).

3.4 Methodology

Hot-start files (fort.68) are first generated for both the KR-G and KR-THR-I meshes by running the ADCIRC model for the prior 61-day period with tidal constituents from the Le-Provost dataset. These files provide the necessary initial conditions for stabilizing tidal simulations. Subsequently, two sets of simulations are performed. The standalone ADCIRC model is

executed for each mesh from May 3 to May 7, 2024 (swell event duration) to isolate the flooding phase effect of the tidal dynamics. Concurrently, the coupled ADCSWAN model is run for the same period to evaluate the combined impacts of tides and waves, with boundary conditions sourced from the WAVEWATCH III model. The SWAN model is initialized using a hot-start file (swan.68) created from a prior 10-day run to ensure accurate initial conditions. The simulation outputs, representing maximum water surface elevation (maxele.63.nc), are downscaled using the Kalpana tool. This downscaling process necessitates additional raster-format input files, such as land use and land cover data (LULC) and a digital elevation model (DEM) specific to the study area, which will be detailed in the following section. The downscaled results from both the standalone ADCIRC model and the coupled ADCSWAN model are then analyzed to evaluate prediction accuracy. To delineate wave-induced impacts, the downscaled results of the standalone ADCIRC model are subtracted from those of the coupled ADCSWAN model. This difference isolates the effects of swells. Finally, the results are compared with field observation data to assess their accuracy and relevance.

3.4.1 Digital Elevation Model

The DEM data for Kerala has a spatial resolution of 30 m (Figure 3.2). It is sourced from the Shuttle Radar Topography Mission (SRTM GL1) Global 30m dataset.
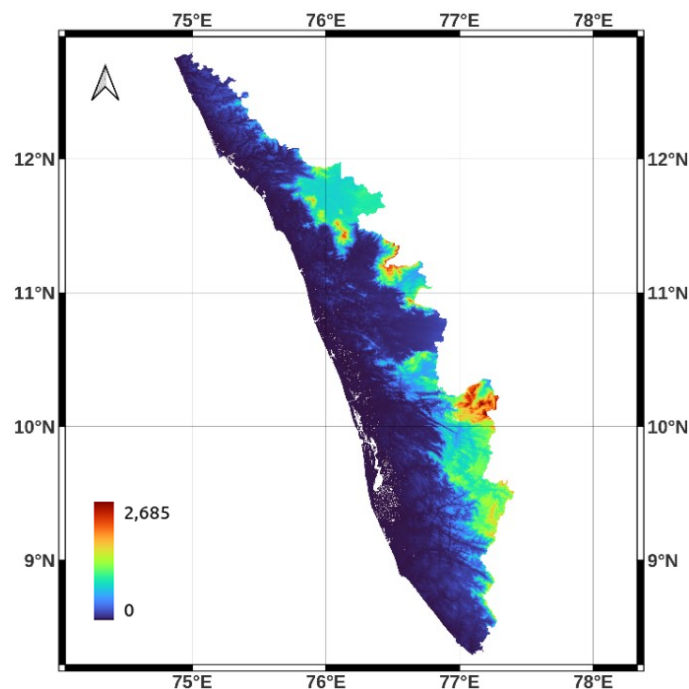

Figure 3.2. Digital Elevation Model of Kerala: SRTM GL1 data with 30-meter resolution.

This DEM, available in Geo-TIFF format through Open Topography, covers the entire Kerala

region and is projected in EPSG:32643 (WGS 84 / UTM zone 43N). It constitutes the principal input for the downscaling methodology.

3.4.2 Land Use and Land Cover

In conjunction with the DEM, the head loss method necessitates land use/land cover (LULC) data to ascertain Manning's roughness coefficients. The LULC dataset employed in this study is derived from ESA Sentinel-2 imagery, offering a spatial resolution of 10 meters and categorized into 11 distinct land cover types (Figure 3.3). This dataset can be accessed through the ESA Sentinel-2 Land Cover Explorer.
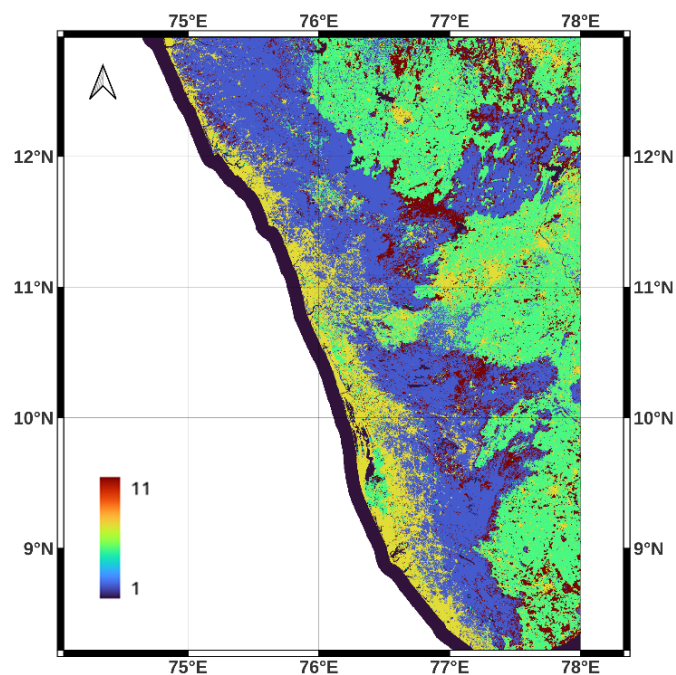
Figure 3.3. Land Use/Land Cover classification for Kerala (2023) derived from ESA Sentinel-2 imagery with 10m resolution

This dataset is available for multiple years as a time series, with the most recent data from 2023 being utilized. The GeoTIFF formatted dataset has been converted to Erdas Imagine (.img) format using QGIS to ensure compatibility with the Kalpana. Discrepancies in resolution between the DEM and the LULC data are addressed by Kalpana through interpolation techniques to ensure consistency.

3.5 Results and Discussions of the May 4, 2024 Swell Event

3.5.1 Tide-only Simulation using ADCIRC

Figure 3.4a illustrates the native ADCIRC simulation results for the KR-THR-I mesh, depicting

the high tide water extent along the Kodungallur coastal stretch, represented in blue. The KR-THR-I mesh results exhibit a resolution discrepancy of approximately 100 m relative to the base map. This shift in the data is due to interpolation issues encountered during the merging of different sources of topography and bathymetry, which can be mitigated by incorporating the coastline as a break line. This improvement will be addressed in future work. Despite this slight offset, it is within acceptable limits, ensuring precise feature identification within a 100 m radius. The results of the Kodungallur stretch were analyzed, focusing on two locations marked in Figure 3.4. The Puthiya Road Beach - Edavilangu Village Extent and the Eariyad - Chandakadappuram Extent experienced inundation during the swell event on May 4, 2024.

Two downscaling methods were employed to improve high tide water extent predictions, with a peak water elevation of 0.4 m observed in the maxele.63 output for the study area.
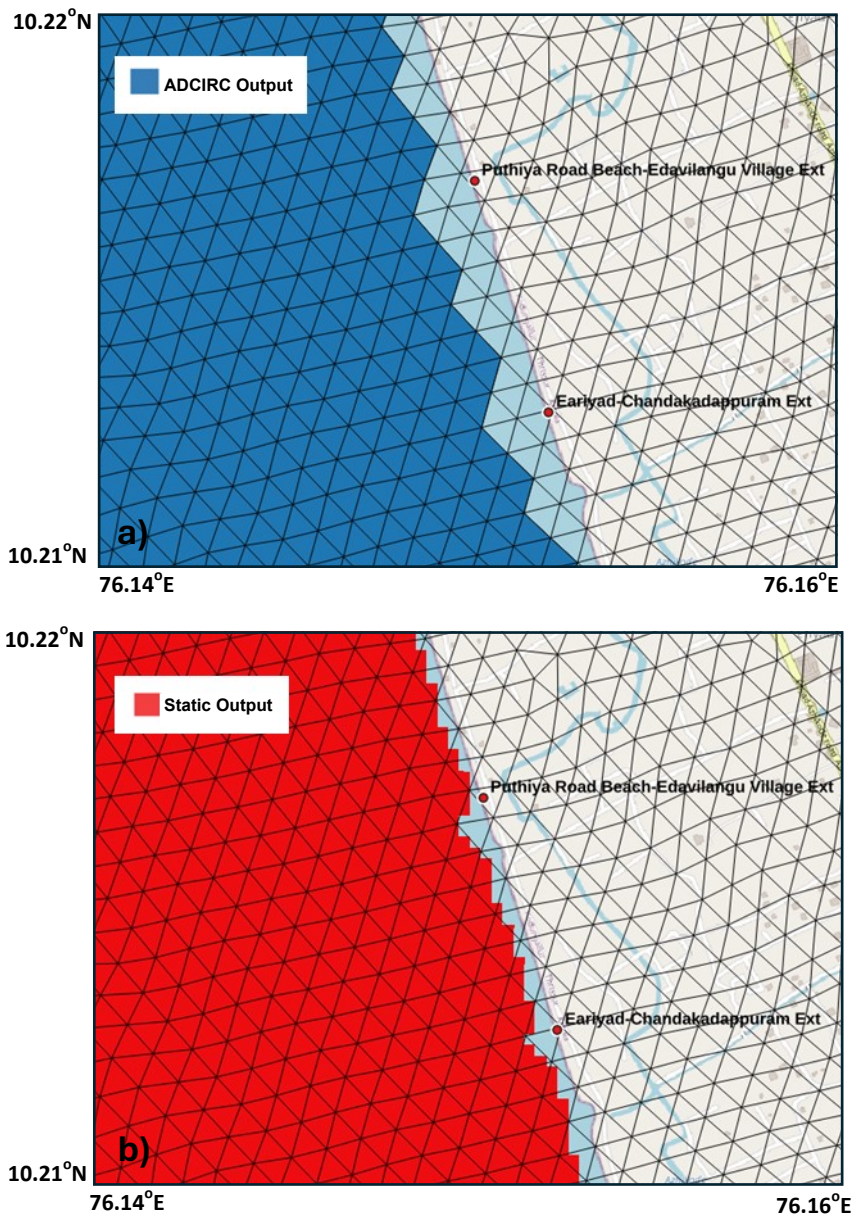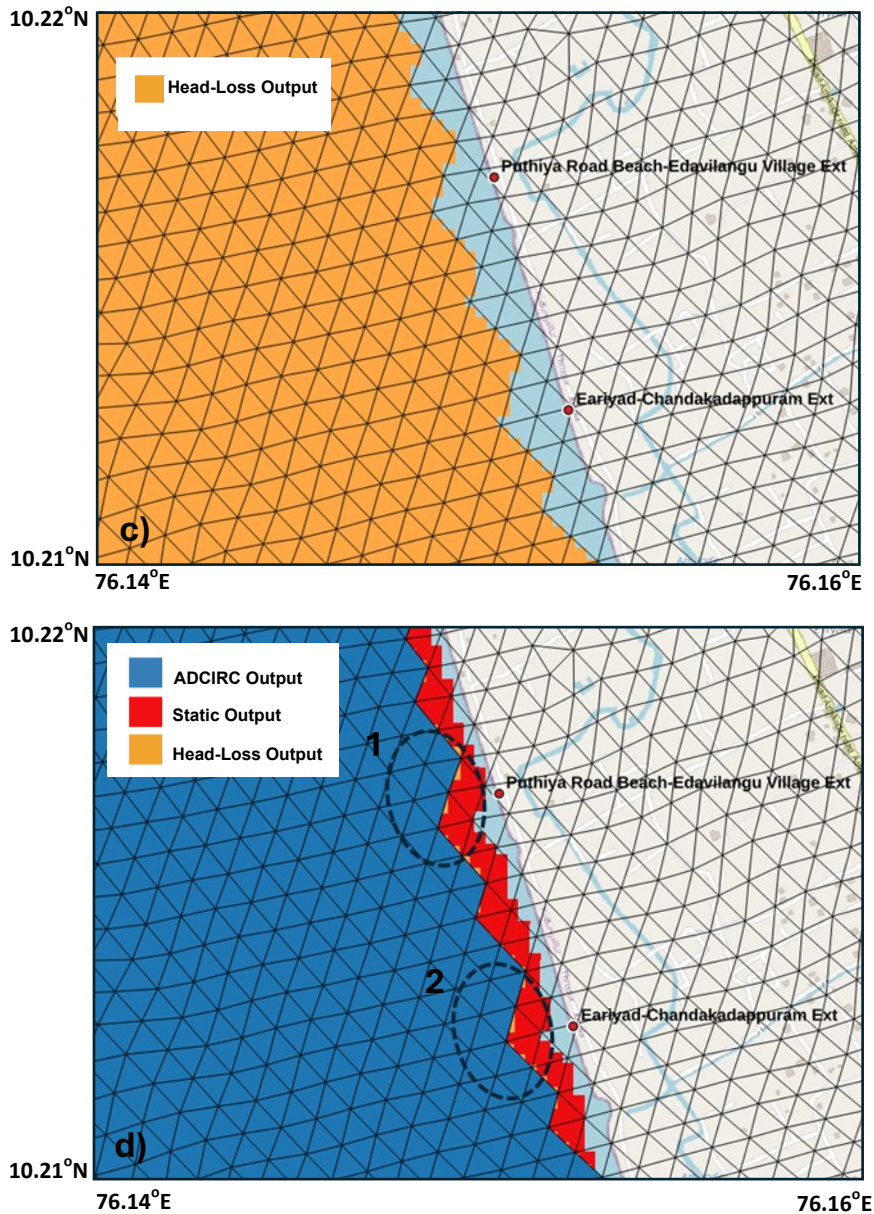
Figure 3.4. High tide water extent in the Kodungallur coastal stretch using the KR-THR-I mesh. The ADCIRC model output is shown in blue, the static output in red, and the head loss method in mustard yellow.

The static method extends this elevation to match the topographic contours (Figure 3.4b). On the other hand, the head loss method integrates LULC data into the cost surface calculation, offering a more precise delineation of the high tide line (Figure 3.4c). LULC data assigns varying resistance values to flow depending on the terrain, with lower resistance for beach slopes and higher for vegetated or densely built areas. This approach accounts for coastal features like seawalls, which prevent inland water penetration, even when the ADCIRC model indicates a surge from tides or waves. Figure 3.4d displays the combined results from both methods, highlighting the difference between the ADCIRC high tide extent and the downscaled

17

outputs. The static method tends to overestimate water extent, while the head loss method, shown in mustard yellow at locations 1 and 2, accurately captures water extent due to the gently sloped beach. It effectively identifies regions where the ADCIRC output underestimates water coverage.
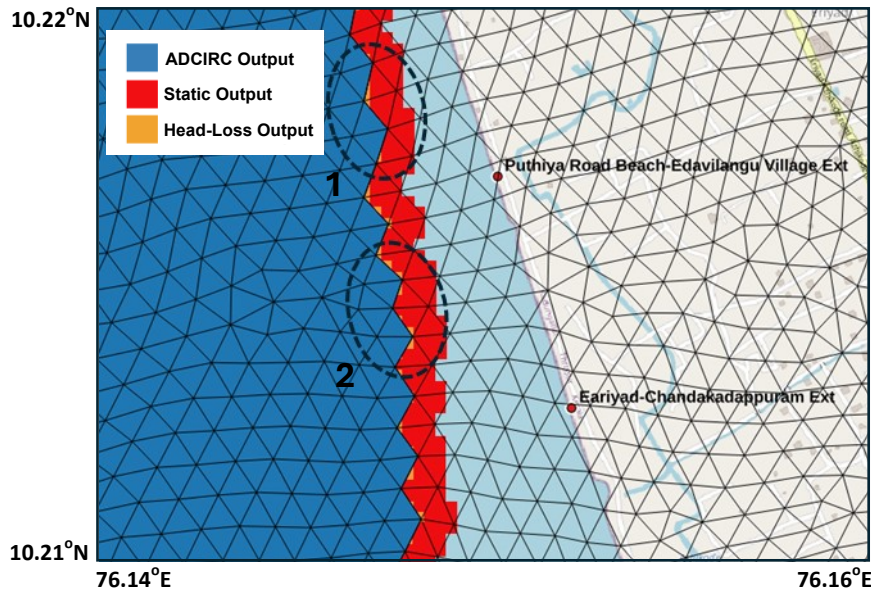

Figure 3.5. Water extent predictions for the KR-G mesh, with ADCIRC (Blue), Static method (Red), and Head-loss method (Mustard yellow).

The KR-G mesh results exhibit a resolution discrepancy of approximately 1,000 m relative to the base map (Figure 3.5). This discrepancy leads the static downscaling method to project the water level contour further inland compared to the KR-THR-I static output (Figure 3.5). The high tide line extents at the observation locations, Puthiya Road Beach - Edavilangu Village and Eariyad – Chandakadappuram, are consistent with the marked locations 1 and 2, respectively, in Figure 3.5. While the head-loss method shows improved accuracy over the static approach, the low-resolution bathymetry introduces significant errors in spatial predictions. Additionally, the smoothed topographic data leads to an overestimation of water extents in certain areas.

Assessment of both mesh models confirms that the head-loss method consistently produces more accurate results than the static method. However, the accuracy of these predictions is highly dependent on the resolution of the coastal relief data used in mesh generation. Consequently, the downscaled outputs from the head-loss method for both meshes will serve as the reference in the subsequent section for analyzing wave-induced water extents.

3.5.2 Wave and Tide Simulation using ADCSWAN

Figure 3.6 displays the predicted water extents for the swell surge event for both KR-THR-I and KR-G meshes, utilizing various downscaling techniques, alongside the native ADCSWAN output. As seen in prior analyses, the static downscaling method generally overestimates inundation, projecting the water line further inland. Conversely, the head-loss method, indicated in mustard yellow at key sites (1 and 2), provides a more accurate representation of observed wave impact areas (Figure 3.6a).
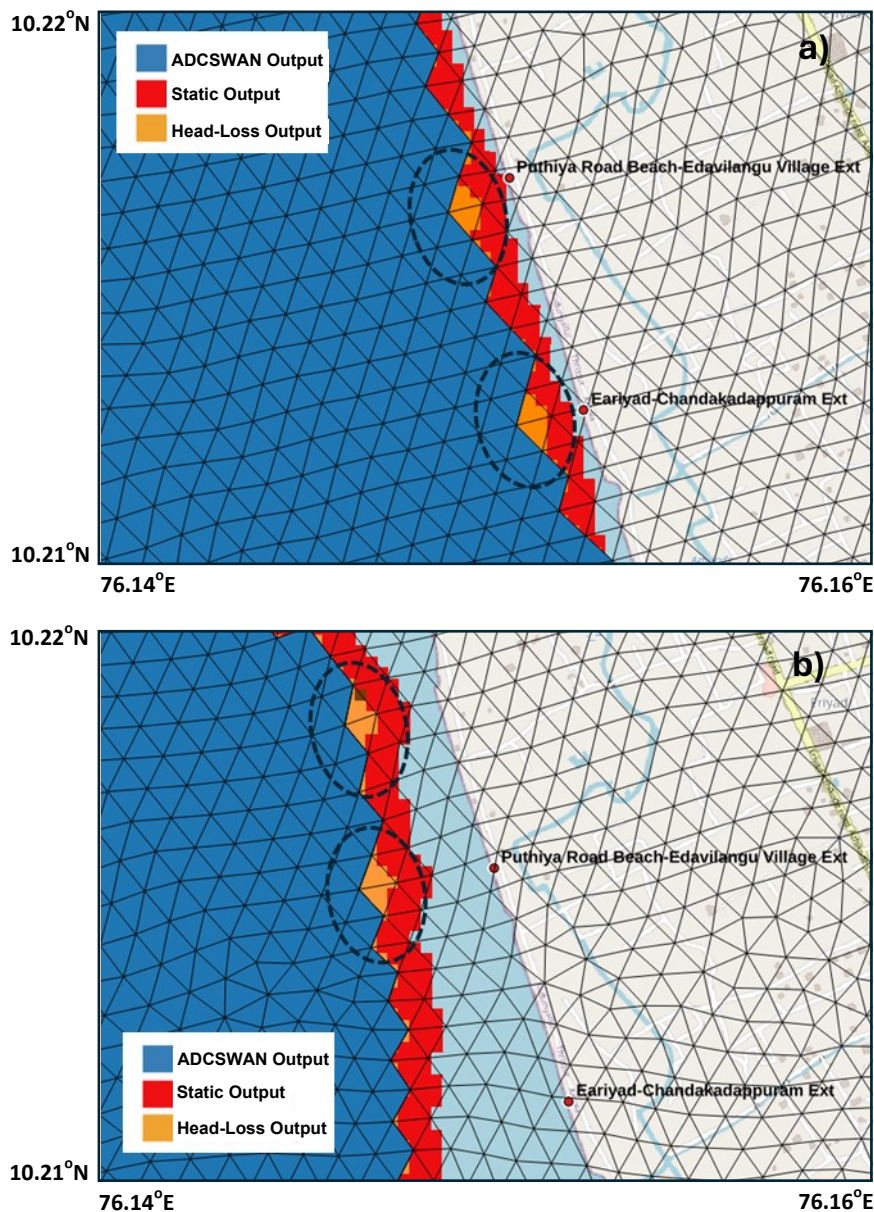

Figure 3.6. Water extent predictions for swell surge event using two meshes: a) KR-THR-I and b) KR-G, with ADCSWAN (Blue), Static method (Red), and Head-loss method (Mustard Yellow).

The KR-THR-I mesh exhibits superior accuracy in delineating inundation extents. Downscaled predictions from the KR-THR-I mesh closely match field observations at sites such as Eariyad-Chandakadappuram and Puthiya Road Beach-Edavilangu Village, with accuracy within a 100-meter radius (Figure 3.6a). This high precision renders the KR-THR-I mesh highly valuable for operational forecasting and timely alert issuance. Conversely, while the KR-G mesh reflects similar inundation features, it demonstrates a notable spatial offset from observed data (Figure 3.6b). This discrepancy hinders precise location identification and complicates the issuance of accurate alerts.

To isolate wave-induced impacts, the tidal water extent predicted by the head-loss method from the ADCIRC model was utilized as a reference baseline. By subtracting this baseline raster data from the coupled ADCSWAN head-loss downscaled output, wave effects were effectively separated. Model predictions were validated against field observations at key locations:

- At the Eariyad-Chandakadappuram extent, the observed inundation was 115 m in extent and 150 m in stretch. The KR-THR-I mesh downscaled data indicated a 95 m extent and a 150 m stretch (Figure 3.7a), while the KR-G mesh showed an 80 m extent and a 130 m stretch.

- For the Puthiya road beach-Edavilangu village extent, observations recorded a 115 m extent and a 200 m stretch. The KR-THR-I mesh reported a 100 m extent and a 130 m stretch (Figure 3.7a), whereas the KR-G mesh displayed an 82 m extent and a 110 m stretch.
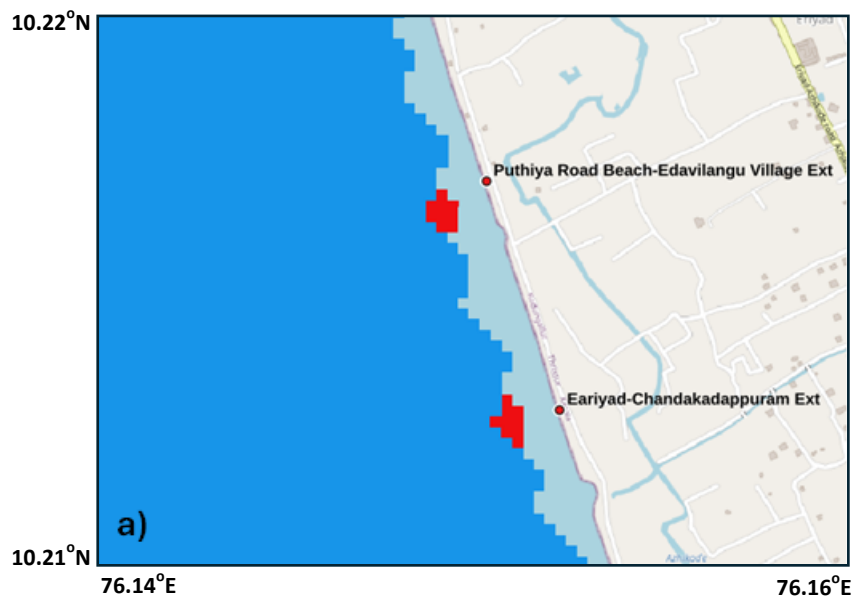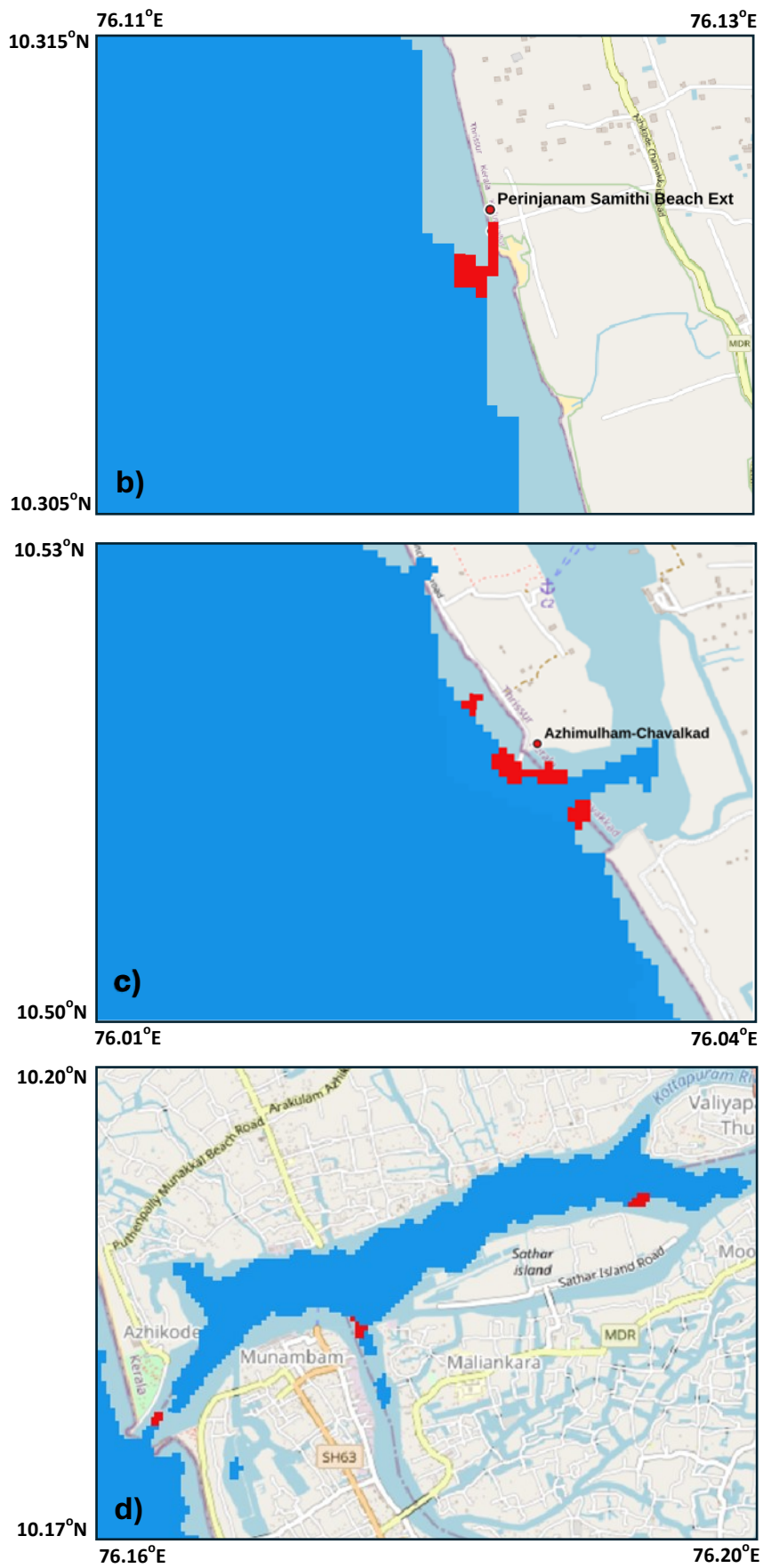
Figure 3.7. Wave-induced flooding patterns for May 4, 2024 event: Red areas represent isolated wave effects.

- At Perinjanam Samithi Beach Extent, the observed inundation extent was 70 m with a 200 m stretch. The KR-THR-I mesh data indicated a 80 m extent and a 190 m stretch (Figure 3.7b), while the KR-G mesh failed to capture any inundation at this location.

Despite some discrepancies in inundation stretch, the KR-THR-I mesh accurately captures the inundation extent and location. This indicates that further refinement with higher-resolution DEMs could improve downscaling accuracy. In contrast, the KR-G mesh exhibits spatial misalignment and fails to detect inundation in certain areas. In certain regions, wave-induced effects captured by the KR-THR-I downscaled output were not reported, likely due to the presence of coastal defenses like seawalls and the lack of nearby population centers. The downscaling technique also showed strong performance in areas such as the estuarine zone of Azhimulham-Chavakkad (Figure 3.7c). It further detected inundation patterns along the Periyar River, notably around Sathar Island, Munnakal Beach, and Munambam stretch (Figure 3.7d). Future alert systems should integrate considerations such as the condition of coastal defenses and the proximity to residential areas to enhance the accuracy and relevance of hazard warnings.

3.6 Results and Discussions of the March 31, 2024 Swell Event

Following the evaluation of the May 4, 2024, swell event, this section presents the results of the March 31, 2024, minor swell event. This event provides additional context for assessing the performance of the modeling system. Consistent with the previous section, the head-loss downscaling technique was used to isolate the effects of swell waves, using the tidal extent from ADCIRC as a baseline to separate wave-induced impacts.

Field observation data were then used to validate this isolated swell wave effect. Notably, field data for the inundation stretch were not collected for this event, which limits the assessment of inundation to the extent only. The KR-G mesh failed to capture swell-induced surge, resulting in the downscaled coupled ADCSWAN output reflecting only the tidal extent without additional inundation from wave impacts. Conversely, the KR-THR-I mesh demonstrated improved performance for this minor event, aligning more closely with field observations.

Downscaled model predictions of KR-THR-I mesh were compared with field observations at key locations:
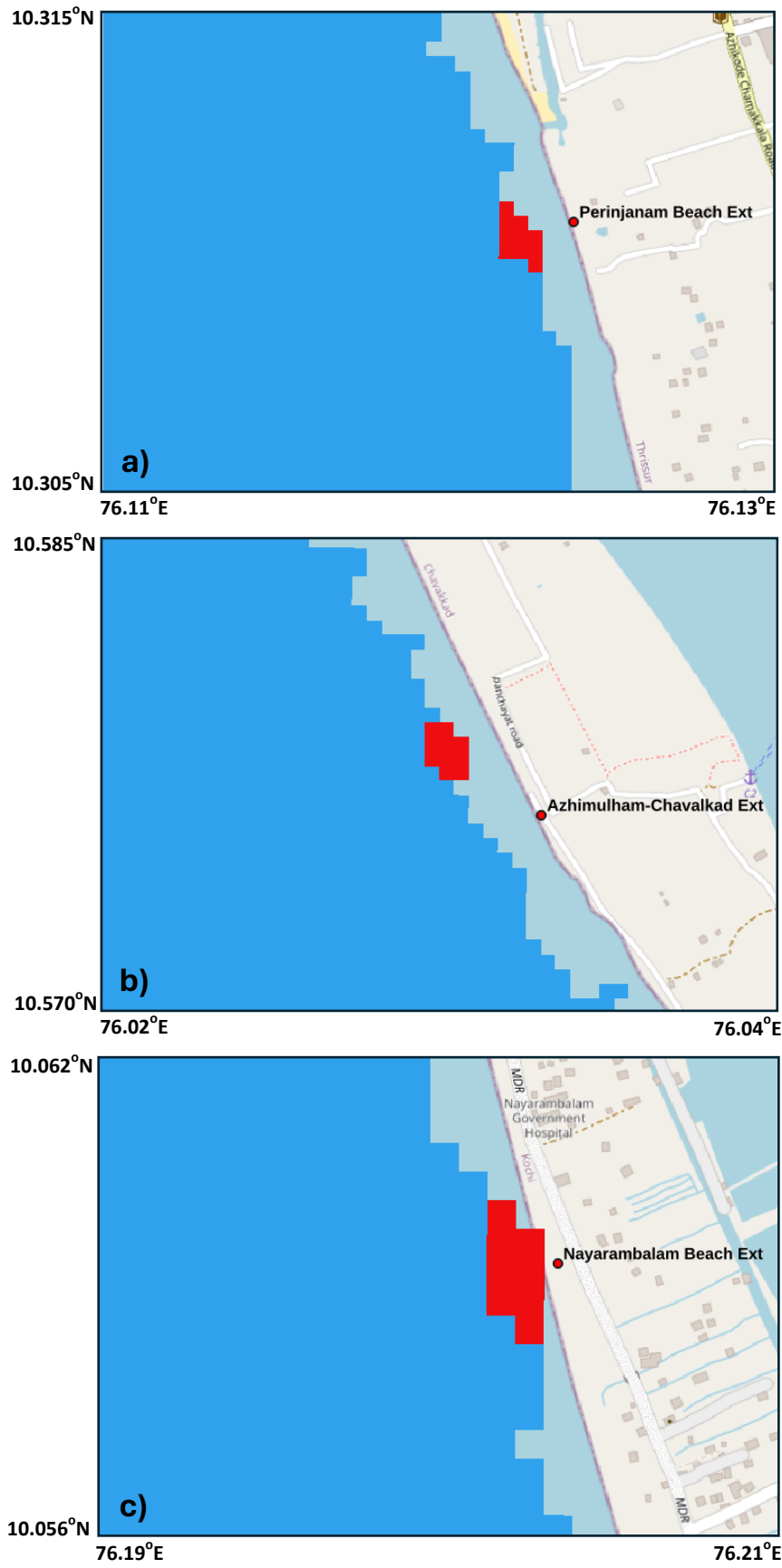
Figure 3.8. Wave-induced flooding patterns for March 31, 2024 event: Red areas represent isolated wave effects

- At Perinjanam Beach extent, the observed inundation extent was 70 m. The KR-THR-I mesh accurately predicted this extent and indicated an inundation stretch of 120 m (Figure 3.8a). However, observational data did not provide measurements of the inundation stretch.

- For Azhimulham-Chavakkad, the observed inundation extent was 30 m. The KR-THR-I mesh overestimated this extent with a predicted value of 80 m and a 250 m offset (Figure 3.8b), likely due to excessive smoothing at the bathymetric-topographic interface. Consequently, the ADCSWAN model exhibited increased wave impact in this area. Since the ADCSWAN model results were already overestimated, the downscaling technique could not reduce the extent; it can only enhance or extend predictions. Additionally, the downscaled model predicted an inundation stretch of 95 m.

- At Nayarambalam Beach, the location was identified as an inundation zone in observations, but specific metrics were not provided. The KR-THR-I mesh accurately located the inundation and predicted an extent of 100 m with a stretch of 160 m (Figure 3.8c).

- At Eriyad village coastal stretch, the ADCSWAN model did not capture the 40 m inundation observed in the field. Examination of the bathymetric-topographic data revealed a sudden steep gradient in the coastal slope. Consequently, the downscaled results could not refine the inundation as no surge was simulated. This underscores the need for improved integration of bathymetric and topographic data to more accurately represent beach slopes and enhance inundation predictions.

The findings confirm that the KR-THR-I mesh is proficient in identifying inundation locations but demonstrates variable accuracy in predicting inundation extent and stretch. In contrast, the KR-G mesh consistently failed to simulate inundation accurately for this minor event. The use of the head-loss method to isolate wave-induced effects from the ADCSWAN output proved effective in distinguishing the impacts of swell waves. Further refinement of bathymetric-topographic data integration is recommended to improve the accuracy of predictions for minor swell-induced flooding events.

4. CONCLUSIONS & FUTURE WORK

Accurate predictions of coastal flooding due to extreme weather events, such as cyclones and high waves/swells, are crucial for effective coastal hazard management and emergency response. However, creating high-resolution simulations over large coastal areas poses computational challenges, often resulting in delays in planning. This study explores the application of downscaling techniques to enhance the resolution of flooding inundation predictions from the coupled ADCIRC+SWAN model.

By leveraging the Kalpana Python module, two downscaling methods, the Static method, and the Head loss method, were evaluated for their effectiveness in refining flood predictions. These downscaling methods were validated against field observations, focusing on the extent, stretch, and location of wave-induced flooding inundations. The findings demonstrate that these techniques can generate high-resolution, accurate flooding inundation forecasts in a timely manner, thereby supporting more effective decision-making during flooding and surge events. The key conclusions of the study are outlined as follows:

- This study successfully applied downscaling methodologies to address micro-scale coastal scenarios, refining high tide line extents and capturing swell wave-induced inundation events.

- The downscaled outputs, particularly those from the Head-loss method, accurately reflect observed wave impact areas. In contrast, the Static method generally overestimates inundation extents.

- The KR-THR-I mesh accurately captures both inundation extent and location, demonstrating its effectiveness for operational forecasting and alert issuance. In contrast, the KR-G mesh displays spatial misalignment and fails to detect inundation in certain areas, highlighting the critical need for accurate high-resolution coastal relief data in mesh generation.

Future studies will explore integrating levee and seawall shapefiles into the head loss downscaling process to enhance flood prediction accuracy. This approach will be tested on additional swell events and cyclonic scenarios to validate and refine the technique.

REFERENCES

1. Booij, N. R. R. C., Ris, R. C., & Holthuijsen, L. H. (1999). A third-generation wave model for coastal regions: 1. Model description and validation. *Journal of geophysical research: Oceans*, 104(C4), 7649-7666.

2. Bunya, S., Dietrich, J. C., Westerink, J. J., Ebersole, B. A., Smith, J. M., Atkinson, J. H., ... & Roberts, H. J. (2010). A high-resolution coupled riverine flow, tide, wind, wind wave, and storm surge model for southern Louisiana and Mississippi. Part I: Model development and validation. *Monthly weather review*, 138(2), 345-377.

3. Cyriac, R., Dietrich, J. C., Fleming, J. G., Blanton, B. O., Kaiser, C., Dawson, C. N., & Luettich, R. A. (2018). Variability in Coastal Flooding predictions due to forecast errors during Hurricane Arthur. *Coastal Engineering*, 137, 59-78.

4. Dietrich, J. C., Tanaka, S., Westerink, J. J., Dawson, C. N., Luettich, R. A., Zijlema, M., ... & Westerink, H. J. (2012). Performance of the unstructured-mesh, SWAN+ ADCIRC model in computing hurricane waves and surge. *Journal of Scientific Computing*, 52, 468-497.

5. Dietrich, J. C., Tull, N., Rucker, C., Langan, T., Mitasova, H., Blanton, B., ... & Luettich, R. (2018, December). Downscaling of Real-Time Coastal Flooding Predictions for Decision Support. *In AGU Fall Meeting* Abstracts (Vol. 2018, pp. NH31C-0988).

6. Dietrich, J. C., Zijlema, M., Westerink, J. J., Holthuijsen, L. H., Dawson, C., Luettich Jr, R. A., ... & Stone, G. W. (2011). Modeling hurricane waves and storm surge using integrally-coupled, scalable computations. *Coastal Engineering*, 58(1), 45-65.

7. Graham, L. et al. (2017). "A Measure-Theoretic Algorithm for Estimating Bottom Friction in a Coastal Inlet: Case Study of Bay St. Louis during Hurricane Gustav (2008)". *Monthly Weather Review 145.3*, pp. 929–954.

8. GRASS Development Team (2017). *Geographic Resources Analysis Support System (GRASS GIS) Software, Version 7.2.* Open Source Geospatial Foundation. URL: http://grass.osgeo. org.

9. Horn, B K P et al. *r.slope.aspect.* Open Source Geospatial Foundation. URL: *https://grass. osgeo.org/grass78/manuals/r.slope.aspect.html.*

10. Larson M, Clements G (2008) r.grow. Open Source Geospatial Foundation, URL: *https://grass.osgeo.org/grass 78/manuals/r.grow.html*

11. Luettich, R. A., & Westerink, J. J. (2004). *Formulation and numerical implementation of the 2D/3D ADCIRC finite element model version 44.* XX (Vol. 20, pp. 74-74). Chapel Hill, NC, USA: R. Luettich.

12. Passeri, D et al. (2011). "Sensitivity of an ADCIRC Tide and Storm Surge Model to Manning's n". *Estuariene and Coastal Modeling,* 4.3, pp. 457–475.

13. Rucker, C. A., Tull, N., Dietrich, J. C., Langan, T. E., Mitasova, H., Blanton, B. O., ... & Luettich, R. A. (2021). Downscaling of real-time coastal flooding predictions for decision support. *Natural Hazards*, 107, 1341-1369.

14. Shapiro M, Clements G (1991) r.mapcalc. Open Source Geospatial Foundation, URL: *https://grass.osgeo.org/ grass78/manuals/r.mapcalc.html*

15. Shapiro M, Metz G (2008) r.clump. Open Source Geospatial Foundation, URL: *https://grass.osgeo.org/grass78/ manuals/r.clump.html*

16. Team, GRASS Development. *r.walk.* Open Source Geospatial Foundation. URL: https:// grass.osgeo.org/grass76/manuals/r.walk.html.

17. Tull, N (2018). "Improving Accuracy of Real-Time Storm Surge Inundation Predictions". *Master's thesis. Raleigh, NC, USA: North Carolina State University.*

18. Westerink, J. J., Luettich, R. A., Feyen, J. C., Atkinson, J. H., Dawson, C., Roberts, H. J., ... & Pourtaheri, H. (2008). A basin-to channel-scale unstructured grid hurricane storm surge model applied to southern Louisiana. *Monthly weather review,* 136(3), 833-864.

19. Westerveldt J, Shapiro M (2008) r.reclass. Open Source Geospatial Foundation, URL: *https://grass.osgeo.org/ grass78/manuals/r.reclass.html*

20. Zijlema, M. (2010). Computation of wind-wave spectra in coastal waters with SWAN on unstructured grids. *Coastal Engineering,* 57(3), 267-277.

APPENDIX

A.1 Installation and Setup of Kalpana

A.1.1 Software & Hardware Requirements

1. **Memory:** Minimum 16GB (more is preferable)

2. **Disk Space:** At least 200GB (more is preferable)

3. **Operating System:** Linux (Ubuntu)

4. **Miniconda (Conda Environment):**

   - Installation Instructions:

```
mkdir -p ~/miniconda3
wget https://repo.anaconda.com/miniconda/Miniconda3-latest-Linux-x86_64.sh -O
~/miniconda3/miniconda.sh
bash ~/miniconda3/miniconda.sh -b -u -p ~/miniconda3
rm -rf ~/miniconda3/miniconda.sh
~/miniconda3/bin/conda init bash
~/miniconda3/bin/conda init zsh
```

5. **Python Libraries:**
   - Requirements:

```
cmocean==2.0
dask==2023.2.0
geopandas==0.12.2
matplotlib==3.7.0
netcdf4==1.6.2
pandas==1.5.3
rioxarray==0.13.3
simplekml==1.3.6
scipy==1.10.0
tqdm==4.64.1
loguru==0.7.0
```

6. **Docker:**

- Installation Instructions:

```
using apt installer


To verify docker is installed successfully:
sudo docker run hello-world


Give permissions
sudo groupadd -f docker
sudo usermod -aG docker $USER
newgrp docker


If docker isn't running (run it with root privileges)
sudo su
Systemctl start docker
systemctl enable docker
systemctl restart docker


To run the docker container, check the current docker container ID using:
docker ps -a


Start docker container using
docker start <container-id>


To go to the container
docker attach <container-id>
```

7. **Grass GIS:**

- Installation Instructions:

```
Make sure to go to the official grass website to see if they made changes to
this repository
sudo add-apt-repository ppa:ubuntugis/ubuntugis-unstable
sudo apt update
sudo apt install grass
sudo apt install grass-core
sudo apt install grass-dev
sudo apt install grass-dev-doc
Sudo apt install grass-doc
```

A.1.2 Running Kalpana

1. Non-interactively (Running Docker Image) (Static Method Only):
   - Pull the required docker image using:

```
docker pull tacuevas/kalpana_nc:latest
```

   - Create a folder, place the maxele.63.nc and input files inside it, and navigate to that directory.
   - Run the Docker image:

```
docker run -it -v "$(pwd)":/home/kalpana/inputs tacuevas/kalpana_nc:latest
```

2. Interactively (Running Docker Image):

To copy all files from a directory in local system to docker container:

```
docker cp /directory-in-local-system/. <container-id>:/directory-in-container
```

3. Running Kalpana Natively:

   - Run the downscaling script in any python interface, by deactivating the source and then activating the Conda environment:

```
Source deactivate
conda activate kalpana
```